QUANTITATIVE ANALYSIS OF TRANS FATTY ACIDS IN COOKED SOYBEAN OIL USING TERAHERTZ SPECTRUM **

F. Y. Lian [1,2], H. Y. Ge [1,2], X. J. Ju [3], Y. Zhang [1,2*], M. X. Fu [1,2]

[1] Grain Information Processing and Control, Key Laboratory of Ministry of Education, Henan University of Technology, Zhengzhou, China; e-mail: lfuwork@163.com
[2] Grain Photoelectric Detection and Control, Key Laboratory of Henan Province, Henan University of Technology, Zhengzhou, China
[3] Collaborative Innovation Center of Henan Grain Crops, Zhengzhou, China

A method for the quantitative analysis of trans fatty acids (TFAs) in cooked soybean oil using terahertz (THz) spectrum is developed. The THz spectra of three groups of soybean oil samples that were cooked at different temperatures for various times were measured using a terahertz time-domain spectrum system (THz-TDS) with frequency range of 0.2–1.5 THz. A partial least squares (PLS) regression model based on the whole THz spectrum was constructed to predict the TFAs content in the cooked soybean oil samples. To reduce noise and improve the prediction accuracy of the model, a subinterval PLS (sub-PLS) model based on a part of the THz spectrum was constructed. This sub-PLS had high accuracy in predicting the TFAs content in cooked soybean oil samples (R = 0.987 and RMSECV = 0.956).

Keywords: *terahertz spectrum, trans-fatty acids, quantitative analysis, partial least squares, subinterval partial least squares.*

КОЛИЧЕСТВЕННЫЙ АНАЛИЗ ТРАНСЖИРНЫХ КИСЛОТ В СОЕВОМ МАСЛЕ С ИСПОЛЬЗОВАНИЕМ СПЕКТРОВ ТЕРАГЕРЦОВОГО ДИАПАЗОНА

F. Y. Lian [1,2], H. Y. Ge [1,2], X. J. Ju [3], Y. Zhang [1,2*], M. X. Fu [1,2]

УДК 543.42.062:665.12

[1] Основная лаборатория Министерства образования, Хэнаньский технологический университет, Чжэнчжоу, Китай; e-mail: lfuwork@163.com
[2] Основная лаборатория провинции Хэнань, Хэнаньский технологический университет, Чжэнчжоу, Китай
[3] Совместный инновационный центр зерновых культур провинции Хэнань, Чжэнчжоу, Китай

(Поступила 11 июня 2018)

Разработан метод количественного анализа трансизомеров жирных кислот (ТИЖК) в соевом масле с использованием терагерцовых (ТГц) спектров. ТГц спектры трех групп образцов соевого масла, приготовленных при разных температурах в течение различного времени, измерены с использованием терагерцовой спектральной системы с разрешением во времени (ТГц-TDS) в диапазоне частот 0.2–1.5 ТГц. Для прогнозирования содержания ТИЖК в приготовленных образцах соевого масла построена регрессионная модель по методу частных наименьших квадратов (PLS) на основе всего ТГц спектра. Для снижения шума и повышения точности прогнозирования модели построена субинтервальная модель PLS (sub-PLS), основанная на части ТГц спектра. Эта модель обеспечила высокую точность прогнозирования содержания ТИЖК в приготовленных образцах соевого масла (R = 0.987) и среднее квадратичное отклонение кросс-валидации (RMSECV = 0.956).

Ключевые слова: *терагерцовый спектр, трансизомеры жирных кислот, количественный анализ, метод частных наименьших квадратов, субинтервальная модель частных наименьших квадратов.*

Full text is published in JAS V. 86, No. 5 (http://springer.com/10812) and in electronic version of ZhPS V. 86, No. 5 (http://www.elibrary.ru/title_about.asp?id=7318; sales@elibrary.ru).

Introduction. Edible oil is one of the basic materials maintaining human life. They are often used for cooking, which leads to a gradual loss in their nutritive value and even generates hazardous substances. Therefore, a rapid and accurate method to analyze the quality of edible oil is required. Traditional analytical methods such as gas chromatography [1, 2], gas chromatography-mass spectrometry [3, 4], liquid chromatography [2, 5], and high-performance liquid chromatography [6] are often used to evaluate the quality of edible oil. However, these methods are time consuming and require complicated pretreatment. Spectrum analyses such as Raman [7–9] or near infrared (NIR) [10, 11] are good analytical tools, and have been widely used to assess food safety. However, few researches [12, 13] have focused on the analysis of edible oil quality using terahertz (THz) spectrum. Zhan et al. [12] used principal component analysis (PCA) and support vector machine (SVM) to identify edible or swill-cooked oil, which proved that the developed method is suitable for the rapid identification of swill-cooked oil but did not offer quantitative analysis for a mixture of edible oil and swill-cooked oil. Li et al. [13] used SVM to investigate the four principal nutritional components in edible oil, and the predicted error of classifications is near 0.5%, but also did not offer quantitative analysis.

Terahertz radiation has a frequency range of 0.1 to 10 T (1 T = 10^{12} Hz), and represents the band of electromagnetic wave between microwave and infrared wave. Rapid progress in generating and detecting THz radiation has promoted the development of analytical methods based on the THz spectra [14, 15]. The vibration frequency of many biological molecules is in the THz range, and many molecular types can be identified based on their THz fingerprint spectra [16, 17]. In addition, THz radiation may easily penetrate many nonpolar materials, and it has been particularly used in detecting explosives and illicit drugs [18, 19]. In recent years, the applications of THz spectrum technology in food quality and safety detection have attracted great interest [20]. Lian et al. [21] used terahertz spectrum to identify of three strains of transgenic maize, and the correct identification rate reached 92% using PCA and SVM analysis methods. Ge et al. [22] obtained and analyzed the terahertz spectra of aflatoxin B1 preserved in acetonitrile solutions with concentration ranges of 1–50 and 1–50 lg/L, and used PCR, PLS, and SVM to do a quantitative analysis for the concentration range of 1–50 lg/mL. Jiang et al. [23] proposed a feasible tool that uses a terahertz imaging system to identify wheat grains at different stages of germination. Their experimental results indicated that the THz technology combined with chemometrics could be a new effective way to discriminate the types of measured objects.

The goal of our study was to develop a method to quantify TFAs in cooked soybean oil based on THz spectrum analysis. The THz frequency used in our study is in the range of 0.2–1.5 THz. The THz spectrum data were used to construct a model using the partial least squares (PLS) method to predict the TFAs content in cooked soybean oil. The accuracy of the model was tested by comparing the measured TFAs values with the predicted TFAs values. An optimized sub-PLS model based on the most meaningful part of the THz spectrum was proposed, which has better performance than PLS in predicting the TFAs content in cooked soybean oil.

Data acquisition. The apparatus used in the experiment, the terahertz time-domain spectrum system (THz-TDS) "Z3", made by Zomega Corp., in USA, has been widely applied in materials testing in recent years. The work of THz-TDS is as follows: The mode-locked Ti-sapphire femtosecond laser, which provides 100-fs pulses at a wavelength of 800 nm and a repeating frequency of 80 MHz, is divided into two beams (pump beam and probe beam) using a polarization beam splitter (PBS). The THz pulses are generated from the low-temperature-grown GaAs photoconductive antenna with an attached silicon hyperhemispherical lens. The THz radiation from the emitter is collected and focused on the sample through a pair of parabolic mirrors (PM). Electrooptic (EO) detection is used to detect the THz signal. The transmitted THz radiation is focused and collimated through the PM onto the ZnTe EO detector crystal [24]. The THz beam path should be filled with nitrogen gas to remove absorbed atmospheric water vapor [25]. The samples are placed at the focal point of the THz beam spectroscope, and the measurements are performed at an ambient temperature of 294 K with a relative humidity of approximately 4%.

The THz-TDS can give both the phase and amplitude of the THz pulses for detection. A reference pulse signal, $E_{\mathrm{ref}}(\omega)$, in the absence of sample, and a sample pulse signal, $E_{\mathrm{s}}(\omega)$, are recorded. Comparing the sample pulse and reference pulse using fast Fourier transformation, the complex refractive index $N(\omega)$ can be expressed as follows:

$$N(\omega) = n(\omega) - ik(\omega), \quad (1)$$

where $n(\omega)$ and $k(\omega)$ are the real refractive index and extinction coefficient, respectively, which describe the dispersion and absorption characteristics of the sample, ω is the cyclic frequency, and i is the imaginary unit. The complex transfer function $H(\omega)$of the sample [26], is as follows:

$$H(\omega) = \frac{E_s(\omega)}{E_{ref}(\omega)} = \frac{4N}{(N+1)^2} \exp\left(\frac{i\omega(N-1)d}{c}\right) = \rho(\omega)\exp\left(i\varphi(\omega)\right), \quad (2)$$

where $E_s(\omega)$ and $E_{ref}(\omega)$ are the complex amplitudes of the Fourier transform of $E_s(t)$ and $E_{ref}(t)$, respectively, c is the speed of light, and $\rho(\omega)$ and $\varphi(\omega)$ are the amplitude ratio and related phase difference of the reference and sample, respectively.

The $n(\omega)$ and absorption coefficient $a(\omega)$ can be obtained using the equations

$$n(\omega) = [\varphi(\omega)/\omega d]c + 1, \quad (3)$$

$$a(\omega) = \frac{2}{d}\ln\left(\frac{4n(\omega)}{\rho(\omega)(n(\omega)+1)^2}\right). \quad (4)$$

Sample preparation. In this research, samples were bought from the supermarket, and their compositions are as follows: saturated fat 16.0 g/100 g, monounsaturated fat 25.0 g/100 g, polyunsaturated fat 59.0%, cholesterol 0%, carbohydrate 0%, and protein 0%. The fresh soybean oil does not contain trans-C18:1, but contains small amounts of *trans*-C18:2 and *trans*-C18:3. The samples were heated at 160, 180, and 200°C for 15 min, 0.5 h, 1, 2, 4, 8, and 12 h using crucibles. In total, 480 samples including the unheated were prepared for testing.

The 480 samples were divided into three groups by average, and each group was heated at 160, 180, and 200°C. In addition, each group contains additional 20 unheated samples besides the heated samples. In each group, 80 samples randomly selected formed the calibration set, and the rest of 80 samples formed the prediction set. When preparing samples, disposable SiO_2 cuvettes with an optical path of 1 mm were used. The samples were prepared at room temperature and measured within one day to avoid contamination from the environment.

PLS and Sub-PLS. Partial least squares (PLS) regression is an optimization tool for quantitative analysis, which has been widely applied in different fields [27–30]. Some latent variables in PLS regression represent the maximal covariance between matrices [31]. By using PLS in this research, the best correlations between the spectral data X and Y that measured for TFAs in cooked soybean oil are as follow:

$$X = TP^T + E, \quad Y = UQ^T + F,$$

where X is the input matrix and Y is the output matrix, T and U are the score matrices, P and Q are the loading matrices that represent the covariance between X, Y, and U, respectively, and E and F are the residual matrices. In our research, the input matrix X was derived from the absorption coefficient and refractive index within a selected frequency range of THz, and the TFAs content in measured samples formed the output matrix Y.

In the experiments, the TFAs content was divided into eight ranges for quantitative and predictive analyses: 1) TFAs range 0.30–0.44, 2) 0.45–0.59, 3) 0.60–0.74, 4) 0.75–0.89, 5) 0.90–1.04, 6) 1.05–1.19, 7) 1.20–1.34, 8) over 1.34%. The reason why we classified TFAs into different levels is that we need a criterion that determines whether the predicted result is correct using our model. If the predicted value is in the correct range, the predicted result is correct.

The whole THz spectrum of each sample usually included some noise regions, which reduced the reliability of analysis. To improve reliability and simplify calculation, we selected the best area to replace the whole spectrum to perform PLS. This is the method known as subinterval PLS (Sub-PLS). Therefore, the whole spectrum was divided into several subintervals with equal width for comparison. The best subinterval was selected in accordance with the root-mean-square error (RMSE) of cross-validation (RMSECV) value. Both the Sub-PLS model and the PLS model were evaluated by comparing the correlation coefficient (R) between the measured value and the predicted value, the root-mean-square error of the calibration set (RMSEC), and that of the prediction set (RMSEP). The best model is the one that has the highest R value and the lowest RMSE value. The above parameters can be calculated as follows:

$$\mathrm{RMSECV} = \sqrt{\frac{1}{n}\sum_{i=1}^{n}(y_r^i - y_p^i)^2}, \quad (5)$$

$$R = \frac{\sum_{i=1}^{n}(y_{\mathrm{r}}^{i} - \bar{y}_{\mathrm{r}})(y_{\mathrm{p}}^{i} - \bar{y}_{\mathrm{p}})}{\sqrt{\sum_{i=1}^{n}(y_{\mathrm{r}}^{i} - \bar{y}_{\mathrm{r}})^{2}\sum_{i=1}^{n}(y_{\mathrm{p}}^{i} - \bar{y}_{\mathrm{p}})^{2}}}, \quad (6)$$

where n is the number of samples in the calibration set, y_{r}^{i} is the reference value of the ith sample, y_{p}^{i} is the predicted value of the ith sample, $\bar{y}_{\mathrm{r}}$ is the average of the reference values, and $\bar{y}_{\mathrm{p}}$ is the average of the predicted values.

Experimental results and discussion. To increase the signal-to-noise ratio (SNR), each sample was measured three times using THz-TDS. The spectrum of each sample was the average of three scanning results, and the reference spectrum was also measured after every three scans. The effective THz testing frequency is in the range of 0.2–1.5 THz. The typical THz time-domain spectra of the partial samples are shown in Fig. 1a. Their corresponding frequency-domain spectra that were obtained using fast Fourier transform are shown in Fig. 1b. The refractive indices and the absorption coefficients of the samples were calculated using Eq. (3) and Eq. (4), as shown in Fig. 1c,d.

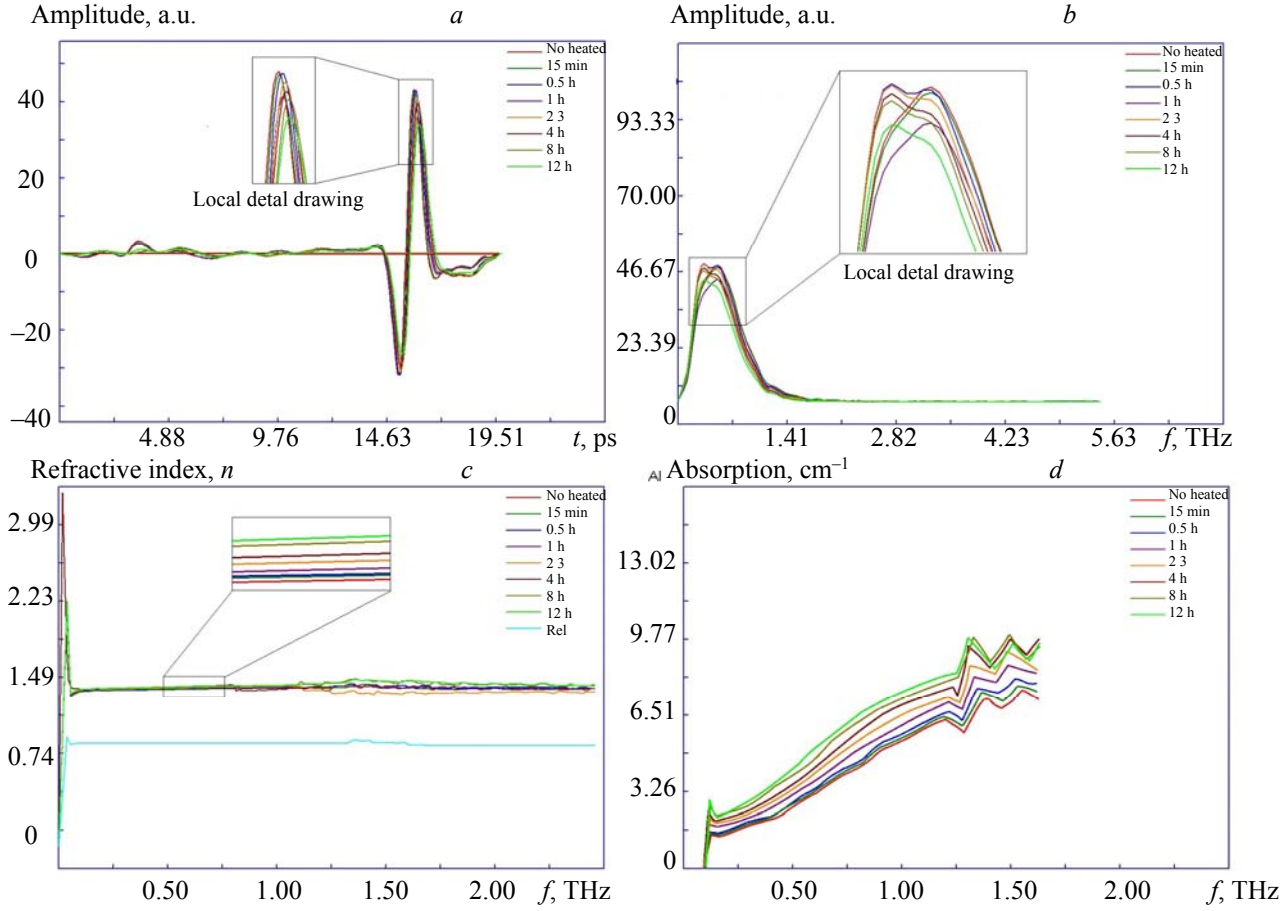

Fig. 1. THz time-domain spectra (a), frequency spectra (b), refractive index spectra (c), and absorption spectra (d) (samples were heated at 180°C for half an hour).

Spectrum analysis. As shown in Fig. 1, there was an effective narrow bandwidth (about 0.2–1.5 THz) in the entire measurement range of 0.1–2.25 THz. Although the difference in the spectral shape among the samples was not obvious, we can still find their differences after being amplified in the effective bandwidth. Particularly, Fig. 1c illustrates some significative differences in the refractive indices between samples. Moreover, Fig. 1d shows that the differences in the absorption spectral shapes among samples indicate that there are some differences in the THz absorption coefficients. In particular, we have already adjusted the

experimental system to optimal signal-to-noise ratio (10^4) terahertz range in the used, and several experiments also proved good stability and repeatability of the experimental system. Therefore, we can basically avoid the influence caused by measuring error for the above results.

Because all of the samples contained similar components, their optical parameters were very closed to each other, as shown in Fig. 1a,b. To enhance the differences among spectra, the average values of the absorption coefficient of eight levels of TFAs content at certain temperatures were calculated. For example, at 180°C, the computed average values of the absorption coefficient of each level were 3.84, 3.93, …, 5.24. In addition, because of the limitation of the dynamic range of THz-TDS, there was a lower SNR in the higher frequency region of the spectra (>1.5 THz) in all samples. Because there were no distinct absorption peaks in the spectra and the differences in spectra among samples were not obvious, we used a PLS regression to investigate the relationship between the changes in the chemical properties of the samples and their spectra.

PLS analysis. Using the PLS toolbox (version 4.0, Eigenvector Research Inc., Wenatchee, WA, USA) in the MATLAB software package (version 2013a), three groups of soybean oil samples were analyzed. The eight levels in each group were assigned numbers from 1 to 8 (Table 1) as output variables, and the original spectra of the samples were used to establish the PLS model. Then, the PLS calibration model was developed using a leave-one-out cross-validation calculation. To obtain the best model, the typical range from 0.2 to 1.5 THz was applied. The aim of the PLS model was to predict which level of TFAs a new sample contains. We used 480 samples to construct the prediction model. All the samples in each group were also split into two small groups randomly: the calibration set (80 samples) and the prediction set (80 samples). The performance of the model is summarized in Table 1.

TABLE 1. Calibration and Validation Results from PLS Model based on the Range of 0.2–1.5THz

Variable used	Calibration		Cross validation	
	R	RMSEC	*R*	RMSECV
Absorption coefficient	0.979	0.833	0.976	1.093
Refractive index	0.973	1.374	0.968	1.427

Note: the above results are from experimental results using THz-TDS.

Compared to the PLS model based on the refractive index, the PLS model based on the absorption coefficient possessed the lower RMSE value and the higher R-value, which indicated better performance. Thus, the PLS model based on the absorption spectrum predicted the TFAs content of soybean oil more accurate than that based on the other spectrum in the THz frequency range of 0.2–1.5 THz.

Figure 2 shows a comparison between the predicted results and the measured results at each specified temperature using the THz absorption spectrum-based PLS regression model. The predicted values of TFA content of all samples were consistent with their measured values, which indicated that the PLS model was effective for the quantitative analysis of TFAs in cooked soybean oil.

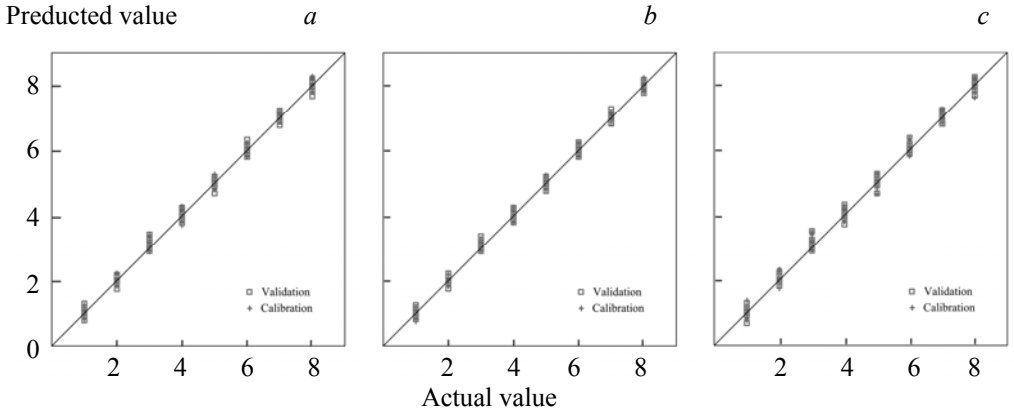

Fig. 2. Relationship between the measured values and the predicted values using PLS model at 160 (a), 180 (b), and 200°C (c).

Sub-PLS analysis. To remove noise and improve the performance of the model, we developed a sub-PLS model based on the former PLS model using the same absorption spectra. First, the full spectrum was divided into 16 equispaced subintervals, and calibration models were built for each subinterval (in total, 16 models). Then, cross-validation was performed for each of the 16 sub-PLS models. Figure 3 shows the RMSECV value for each model and the mean absorption spectrum. Each column, which represents a sub-PLS model, has the same width, and its height indicates the RMSECV value of the corresponding model. Sub-PLS model No. 8 with the frequency range of 0.788–0.900 THz has the lowest RMSECV value, so it was selected as the best subinterval for building the sub-PLS model.

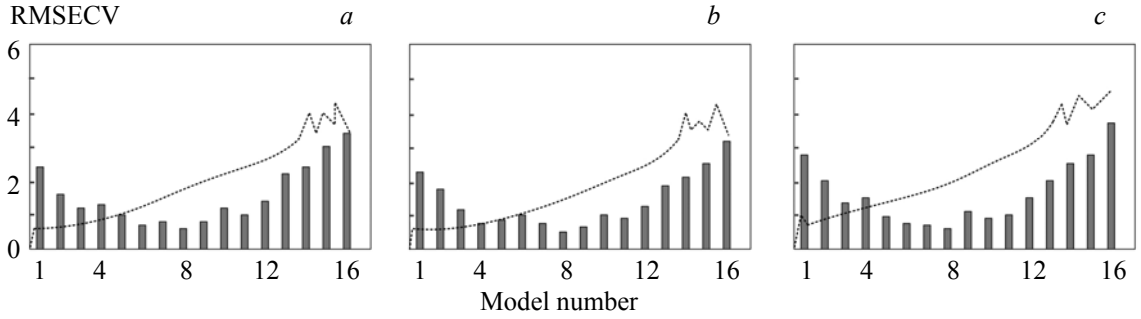

Fig. 3. RMSECV values of each sub-PLS model and mean absorption spectrum at 160 (a), 180 (b), and 200°C (c).

The most useful part of the whole spectrum to estimate TFAs content was selected to enhance the performance of the model. In general, the most useful part of the spectrum is the one with the lowest RMSECV. In our experiment, we divided the whole spectrum into 32, 16, and 8 subintervals, and used three widths (4, 8, and 16) to build some sub-PLS models. The calibration and validation values of the optimal sub-PLS models are shown in Table 2.

TABLE 2. Parameters of Optimal Sub-PLS Regression Models under Three Sub-interval Widths

Subinterval width	Frequency, THz	*R*	RMSEC	RMSECV
16	0.668–0.993	0.981	0.912	1.196
8	0.788–0.900	0.987	0.679	0.956
4	0.774–0.949	0.985	0.863	1.238

As shown in Table 2, the sub-PLS model with width of 8 shows lower RMSECV and RMSE values and higher *R* value than those of the other Sub-PLS models and the full spectrum PLS model (Table 1). These results indicated that the Sub-PLS with an appropriate subinterval showed better performance for classification than the full-spectrum PLS model. A note about *R* parameter is that a higher *R* value does not necessarily indicate a fit model, but experiments show that it is appropriate for evaluating our model.

Figure 4 compares the measured values with the predicted values using the full-spectrum PLS model and the optimal sub-PLS model with the frequency range of 0.788–0.900 THz. The RMSEP of the full-spectrum PLS model is 0.861, while that of the sub-PLS model is 0.639. The eight subintervals along the *X*-axis represent the eight levels of TFAs content (No. 1–8) in fresh soybean oil samples and those that were heated for 15 min, 0.5 h, 1.0, …, and 12 h. The *Y*-axis represents the predicted values from the sub-PLS and PLS models for each TFAs content level. As shown in Fig. 4, the sub-PLS model possesses the maximum estimation range of 0.65–1.05 THz, which is smaller than that of the PLS model (0.60–1.10 THz). This indicates that the sub-PLS model gives better performance is estimating the TFAs content in soybean oil samples, though the degree of dispersion is relatively high in some samples.

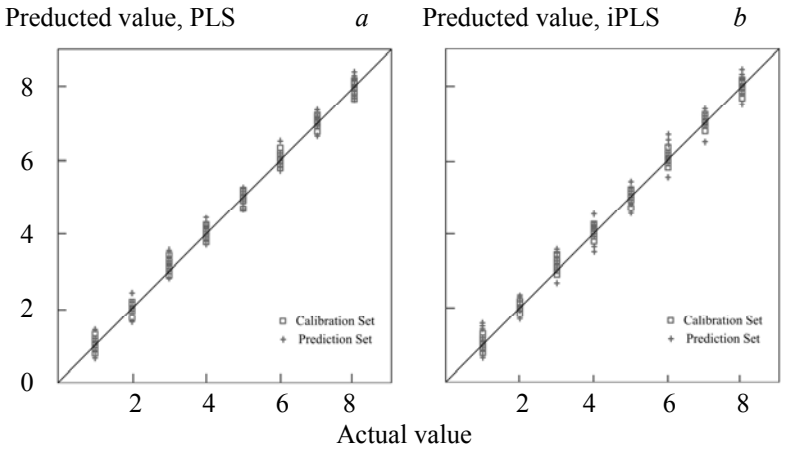

Fig. 4. Scatter plots of the measured values and the predicted values using the sub-PLS model with the range of 0.788–0.900 THz (a) and the full-spectrum PLS model (b).

Detection for samples with unknown temperature. In addition, due to the restrictions of objective conditions, we did not have enough samples for modeling. But it should be pointed out that the model is not intended to detect the temperature of soybean oil but to detect the level of TFAs in soybean oil. To obtain different contents of TFAs of soybean oil, we heated samples at three kinds of temperature. For the samples with unknown temperature, we first used liquid chromatography to determine their contents of TFAs, then entered their spectral data into the Sub-PLS model to predict their levels of TFAs. The experimental results from 100 samples indicated that, compared to the other conventional methods such as support vector machine (SVM), backward propagation neural network (BPNN), and radial basis function neural network (RBFNN), we still obtained excellent prediction results using the proposed Sub-PLS model, as shown in Table 3.

TABLE 3. Prediction Accuracy of the Different Models

Model	Total prediction accuracy, %
SVM	93.00
BPNN	90.00
RBFNN	92.00
PLS	91.00
Sub-PLS	95.00

Like the NIR [10, 11] and Raman spectrum [7–9], the THz spectrum is also a kind of nondestructive and rapid analysis method, but it has better penetrability to our samples. Thus, it is more suitable to construct models to predict the TFAs content in soybean oil. In our experiment, the total time to prepare, measure, and analyze samples was less than 10 min, much less than other traditional biochemical detection methods. Furthermore, the average RMSEP was also lower than that of the method based on NIR spectra (0.31%) that measures using an infrared spectrometer [11]. However, so far, few studies have compared the performance of the PLS model with that of the sub-PLS model in predicting the TFAs content of cooked soybean oil.

Because of the multifarious biomacromolecules in cooked soybean oil, overlapping signals can obscure the THz absorption spectra and lead to a lack of characteristic absorption peaks, and this leads us to the difficult of identifying them in the THz frequency range. In fact, it is normal for many macromolecular substances to possess featureless THz absorption spectrum [32–34]. However, in our experiments, samples with different TFAs content possess distinguishable absorption spectra that are caused by the different levels of absorption by THz waves. Therefore, as used in analyses of other complex substances using THz spectroscopy, chemometric analysis and PLS regression were combined to predict the TFAs content in cooked soybean oil.

To obtain the prediction model with the best performance, we used both PLS and sub-PLS to construct regression models to discriminate the TFAs content in cooked soybean oil based on their THz absorption spectra. Previous studies have shown that the performance of the models can be improved by selecting

a THz subinterval with appropriate range and width. If the subinterval width is too large, irrelevant information and noise will be included, and this may decrease the performance of the models. Because the PLS model uses the full spectrum including noise and irrelevant subintervals, its performance in predicting TFAs content is inferior to that of the optimum sub-PLS model. However, if the subinterval width of the sub-PLS model is too narrow, the prediction error will increase because of the loss of signature information in the spectrum.

The prediction accuracy of the proposed model using THz spectra can be affected by many factors. The THz spectrum of a sample is not only affected by the experimental environment, background noise, and instability of THz-TDS [35], but also by the chemical components of the sample itself. Differences in oil extraction technique, soybean variety, and production area can also result in different proportions of fatty acids and/or various impurities in soybean oil samples, which also affect the THz-TDS spectra. To construct a suitable PLS regression model to predict the TFAs content in cooked soybean oil using THz spectra, other factors that affect THz spectra, such as those mentioned above, should be considered in future research.

Conclusion. In this research, we evaluated the application of the THz spectrum combined with various models and estimated the TFAs content in cooked soybean oil. First, the TFAs content in 480 cooked soybean oil samples was detected and analyzed based on their THz spectra measured in the range of 0.2–1.5 THz in transmission mode. Then, the PLS regression model was constructed to estimate the TFAs content in cooked soybean oil. To improve the prediction performance, the sub-PLS model was developed based on a subinterval (0.788–0.900 THz) of the full spectrum. The experimental results showed that both regression methods had low RMSECV and high *R*-values, which indicate their good prediction accuracy of TFAs content. The sub-PLS regression model (R = 0.987, RMSECV = 0.956) had better prediction performance than the PLS model. Therefore, THz spectroscopy associated with chemometric techniques show good potential to determining the TFAs content in cooked soybean oil. In future work, other factors that affect the THz spectra, such as the oil extraction technique, soybean variety, and production area will be considered to develop better prediction models. The results of this paper show that THz spectrum combined with an appropriate PLS model can be used for quantitative analysis of TFAs in cooked soybean oil.

Acknowledgment. This work was supported by the Open Fund of the Key Laboratory of Grain Information Processing and Control (Henan University of Technology, KFJJ-2017-108), Ministry of Education, Zhengzhou, China, the Fund of Foundation and Frontier of Henan Province (Grant No. 152300410079), Zhengzhou, China, and the Fund of Zhongyuan Scholar of China (172101510005).

We thank Jennifer Smith, PhD, from Liwen Bianji, Edanz Group China (www.liwenbianji.cn/ac), for editing the English text of a draft of this manuscript.

The authors declare no conflict of interest.

REFERENCES

1. R. Ascensión, S. Isabel, C.V. Carmen, *J. Chem.*, **2014**, No. 38, 1–8 (2015).
2. J. M. Cortés, R. Sanchez, A. Vazquez, *J. Agric. Food Chem*., **54**, No. 19, 6963 (2006).
3. M. G. Qian, H. Zhang, K. Z. Jiang, *Food Chem.*, **166**, 23–28 (2015).
4. M. A. Hossain, S. M. Salehuddin, *Arab. J. Chem*., **5**, No. 3, 391–396 (2012).
5. D. Caroline, T. Angélique, S. Louise, *Food Anal. Methods*, **8**, No. 6, 1425–1435 (2015).
6. C. X. Yuan, Y. Y. Xie, Y. X. Ju, *Food Anal. Methods*, **10**, No. 11, 1–7 (2017).
7. Y. Tehseen, D. W. Sun, J. H. Cheng, *Trend. Food Sci. Technol.*, **62**, 177–189 (2017).
8. A. Ahmet, O. A. Swesi, B. S. Alhatab, *J. Mol. Struct.*, **1128**, 590–605 (2017).
9. B. Muik, B. Lendl, *Chem. Phys. Lipids*, **134**, No. 2, 173–182 (2005).
10. X. P. Fu, Y. B. Ying, *Crit. Rev. Food Sci. Nutr.*, **56**, No. 11, 1913–1924 (2016).
11. H. Azizian, J. K. G. Kramer, *J. Am. Oil Chem. Soc.*, **89**, No. 12, 2143–2154 (2012).
12. H. Zhan, J. Xi, L. Xiao, *Food Control*, **67**, 114–118 (2016).
13. J. Li, *IEEE Trans. Instrum. Meas.*, **59**, No. 8, 2094–2098 (2010).
14. F. S. Vieira, C. Pasquini, *Anal. Chem.* **86**, No. 8, 3780–3786 (2014).
15. B. Ferguson, X. C. Zhang, *Physics*, **1**, No. 1, 26–33 (2002).
16. F. Zhao, S. M. Long, Y. Zhang, *Acta Phys. Sin.*, **64**, No. 2, 24202 (2015).
17. E. Hérault, F. Garet, J. L. Coutaz, *IEEE Trans. Terahertz Sci. Technol.*,**6**, No. 1, 12–19 (2016).
18. J. S. Melinger, N. Laman, D. Grischkowsky, *Appl. Phys. Lett.*, **93**, No. 1, 44 (2008).
19. M. Y. Liang, J. L. Shen, G. Q. Wang, *J. Phys. D*, **41**, No. 13, 135306 (2008).

20. K. Q. Wang, D. W. Sun, H. B. Pu, *Trends Food Sci. Technol*., **67**, 93–105 (2017).
21. F. Y. Lian, D. G. Xu, Y. Zhang, *IEEE Trans. Terahertz Sci. Technol.*, **7**, No. 4, 378–384 (2017).
22. H. Y. Ge, Y. J. Jiang, S. H. Xia, *Food Chem*., **209**, 286–292 (2016).
23. Y. J. Jiang, H. Y. Ge, S. H. Xia, *Sci. Rep.*, **6**, 21299 (2016).
24. I. Pupeza, R. Wilk, M. Koch, *Opt. Express*, **15**, No.7, 4335–4350 (2007).
25. X. L. Zhao, J. S. Li, *Int. Photon. Optoelectron. Meet.*, **276**, No. 1, 012234 (2011).
26. Y. Zhang, X. H. Peng, X.C. Zhang, *Chem. Phys. Lett*., **452**, No. 1, 59–66 (2008).
27. O. O. Olaoluwa, B. Isa, S. M. Lembe, *Sci. Horticult.*, **199**, 229–236 (2016).
28. D. C. Gu, M. J. Zou, C. H. Xu, *Food Chem*., **229**, 458–463 (2017).
29. H. Y. Ge, Y. Y. Jiang, S. H. Xia, *Sensors*, **15**, No. 6, 12560–12572 (2015).
30. W. K. Jia, D. A. Zhao, C. L. Hu, *Appl. Intellig.*, **43**, No. 1, 176–191 (2015).
31. B. M. Nicolai, K. Beullens, *J. Lammertyn, Postharvest Biol. Technol*., **45**, No. 2, 99–118 (2007).
32. M. Naftaly, R. E. Miles, *Proc. IEEE*, **95**, No. 8, 1658–1665 (2007).
33. F. Zhang, O. Kambara, M. Hayashi, *RSC Adv*., **4**, No. 1, 269–278 (2015).
34. A. I. McIntosh, B. Yang, R. S. *Chem. Phys. Lett*., **558**, No. 2, 104–108 (2013).
35. W. Withayachumnankul, B. M. Fischer, D. Abbott, *J. Opt. Soc. Am. B*, **25**, No. 6, 1059–1072 (2018).